Tunable High-Molecular-Weight Anion-Exchange Membranes for Alkaline Fuel Cells

Yanting Luo, Juchen Guo, Chunsheng Wang,* Deryn Chu

Tunable alkaline anion-exchange membranes based on QPMBV are synthesized using a bottom-up approach, miniemulsion copolymerization, which can incorporate functional groups into the copolymers with designated composition and high molecular weight. The mechanical and electrochemical properties of the obtained QPMBV membranes are tuned by varying the composition. It is found that the ion exchange capacity of the copolymer, the hydrophilicity of the copolymer chains, the molecular weight, and the glass transition temperature of the copolymers are essential to balance the mechanical and OH^- transport properties of QPMBV membranes. QPMBV membrane fuel cells show the best power output and the long-lasting fuel cell performance among the APE membranes in open literature.

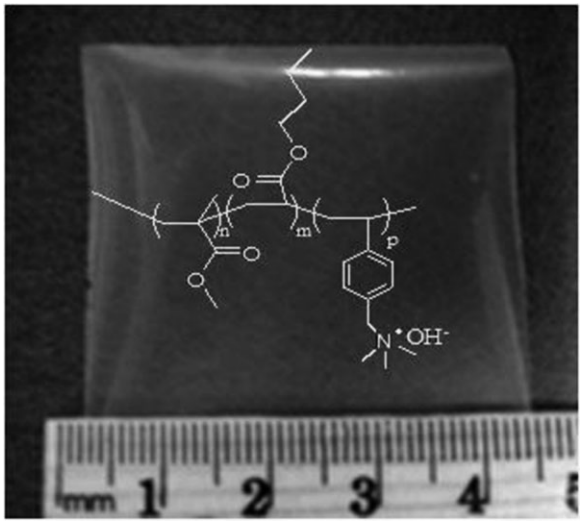

Introduction

The energy crisis has urged the development of more efficient energy conversion technologies including a variety of fuel cells. For the fuel cells operated in low temperatures, typically below 100 °C, there are basically two types of fuel cells distinguished by the different ions being transported in the electrolyte, acid proton-exchange membrane fuel cells (PEMFCs) and alkaline fuel cells (AFCs). Despite the well-recognized good performance of PEMFCs, the investigation on alkaline polymer electrolytes (APEs) for AFCs has been revived recently because of the significant advantages of AFCs over acid PEMFCs in terms of high kinetics for oxygen reduction and fuel oxidation in alkaline environment, and the lower cost by using non-precious metal catalysts.[1]

APE is the key component in an AFC system for transporting hydroxide ions from cathode to anode.[2] APEs with superior conductivity and mechanical strength are of great importance to commercialize the AFC technology. However, APEs still remain in their infancy compared to the commercialized proton exchange membranes such as Nafion. Usually, APEs can be classified into two types based on different anionic site incorporating mechanisms. In the first type, polymeric materials are only used as the matrix to hold KOH solution. Intrinsically, there is no anionic conductive group anchored on the polymer backbone. Hydrophilic polymers including poly(ethylene oxide) (PEO),[3] poly(vinyl alcohol) (PVA),[4] and poly(acrylic acid) (PAA)[5] were often used in this type of APEs. An obvious drawback of these APEs is that they could not eliminate metal ions in the electrolyte. The conductivity of these APEs will be ceased as the OH^- ion being depleted, and the metal ions can easily react to CO_2 in the system to decrease the

Y. Luo, Dr. J. Guo, Prof. C. Wang
Department of Chemical and Biomolecular Engineering, University of Maryland, College Park, MD 20742, USA
E-mail: cswang@umd.edu
Dr. D. Chu
Sensors and Electron Device Directorate, U.S. Army Research Laboratory, Adelphi, MD 20783, USA

DOI: 10.1002/macp.201100218

membrane conductivity and eventually obstruct electrode pores. A more promising type of APEs is the alkaline anion-exchange membranes (AAEMs) that are ionomers in which the anionic conductive sites are anchored on the polymer chains, thus eliminating the metal ions. Usually, those ionomers are composed of two functional portions: hydrophobic and hydrophilic parts. The hydrophobic portion could provide the mechanical support to the AAEMs while the hydrophilic portion is usually the anionic sites with OH^- groups to provide conductivity. A problem of ionomer AAEMs is the low conductivity, which is determined by the concentration of the anionic sites incorporated in the polymer. The conductivity will be increased if more anionic sites are attached. Unfortunately, the mechanical strength of the resulted AAEMs will be undermined at the same time due to higher water sorption. Therefore, one great challenge for ionomer AAEMs is to improve the anionic conductivity without sacrificing mechanical properties. Many originally hydrophobic polymers were used as precursors to synthesize ionomer AAEMs, including polymers with phenyl structured backbones such as polysulfone,[6] poly(arylene ether sulfone),[7] poly(ether ketone),[8] poly(ether imide),[9] poly(phthalazinon ether sulfone ketone),[10] poly(ether sulfone) cardo,[11] poly(dimethylphenylene oxide),[12] and polyphenylene.[13] For these phenyl-structured polymers, the AAEMs were prepared by successive chloromethylation and quaternization. These polymer precursors possess great mechanical strength. However, the resulted AAEMs usually suffer from impaired mechanical strength in humidified condition after incorporating anionic sites by chloromethylation and quaternization. It is because that chloromethylation method is not able to precisely control the concentration and the position of anionic sits on the polymer chains. Therefore, balancing conductivity and mechanical strength is a difficult task for those AAEMs. Fluorinated or partially fluorinated polyethylene were also used as AAEM precursors by Varcoe and coworkers.[14] However, the cost of the γ radiation used to incorporate anionic sites was a considerable drawback of these AAEMs.

An ionomer AAEM based on poly-[(methyl methacrylate)-*co*-(butyl acrylate)-*co*-(vinylbenzyl chloride)] (PMBV) was synthesized by us through free radical solution polymerization.[15] Unlike chloromethylation of existing polymers, we synthesized PMBV with various monomers that were intentionally selected to tune the conductive and mechanical strength. In the PMBV copolymer, methyl methacrylate (MMA) composes the hydrophobic part of the polymer chains that give the polymer mechanical support. Butyl acrylate (BA) is also a hydrophobic portion but with lower glass transition temperature (T_g) comparing with MMA to give certain flexibility of the polymer chains. Vinylbenzyl chloride (VBC) is the functional group that can be quaternized and ion-exchanged to provide the conductivity. Despite promising performance of the PMBV we previously synthesized, its composition was hard to be accurately controlled due to the different conversion of these three monomers in solution polymerization condition. Moreover, the mechanical property of our previous AAEM was not satisfactory due to the low-molecular-weight of the copolymer.[15] To be able to tune the copolymer composition and to enhance its mechanical strength, an advanced miniemulsion polymerization technique was employed in this study to synthesize the PMBV with tunable composition and high molecular weight. The relationships between PMBV composition, OH^- conductivity, and mechanical strength were systematically investigated.

Miniemulsion polymerization is a special type of emulsion polymerization technique that enables incorporation of specific functional monomers at designated compositions to balance conductivity and mechanical strength. In miniemulsion polymerization, a miniemulsion is created by applying high shear force to a regular emulsion consisting of monomer droplets in water phase. Figure 1 illustrates the mechanism of miniemulsion polymerization system. The significant difference between miniemulsion and emulsion is the much smaller and more uniform

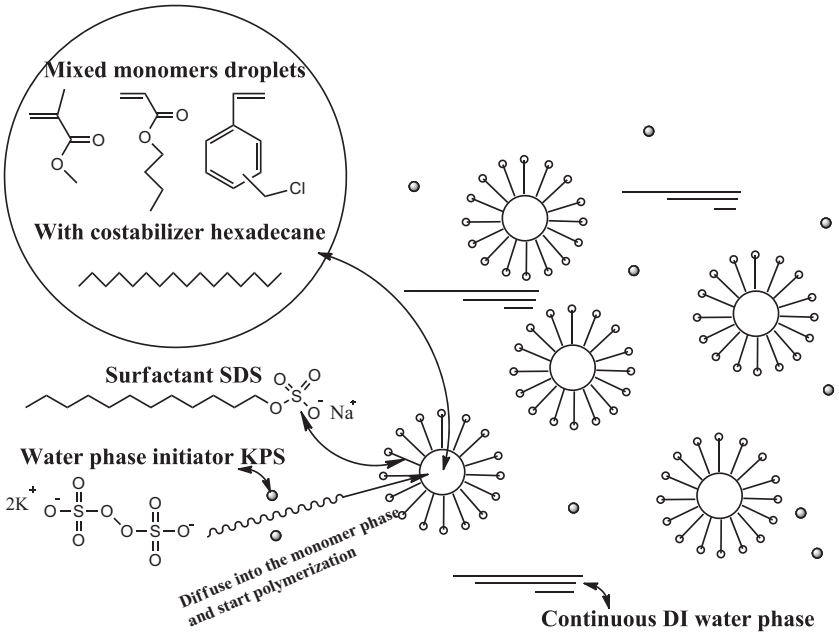

Figure 1. Schematic representation of miniemulsion copolymerization system.

droplet size. Most of the surfactant is adsorbed on the droplet surface due to the large surface area.[16] Therefore, the monomer droplets can be stably dispersed in water phase as individual polymerization loci.[17] Polymerization is primarily initiated in the droplets via free radical entering from water phase. As illustrated in Figure 1, the monomer (mixture of MMA, BA, and VBC) droplets are stabilized in water phase by surfactants (sodium dodecyl sulfate) and co-stabilizer (hexadecane) which is an extremely hydrophobic nonreactive reagent. Free radicals are generated by water phase initiator (potassium persulfate). Every monomer droplet can be considered as a micro-reactor in which bulk copolymerization takes place. Therefore, high conversion of all monomers and high molecular weight of PMBV can be achieved.

In this study, the composition of the PMBV copolymer, i.e., the ratio of MMA/BA/VBC, was tuned using miniemulsion polymerization to study its effect on the conductivity and mechanical strength to achieve high performance of AAEM-based AFCs (AAEMFCs).

Experimental Section

Miniemulsion Copolymerization and Polymer Characterization

A miniemulsion was prepared by dispersing mixture of monomers (30 g) with the designed ratio (MMA/BA/VBC mol%) and hexadecane (0.12 g) into aqueous sodium dodecylsulfate (SDS) solution (0.01 mol $\cdot$ L^{-1}, 150 mL) by vigorous agitation while sonication was applied at the same time with a homogenizer (Omni Sonic Ruptor 400) for 9 min. A stable miniemulsion was formed and transferred into a three-necked flask reactor. The polymerization was initiated by injection of initiator potassium peroxydisulfate (KPS, 0.01 mol $\cdot$ L^{-1} of the water phase) into the miniemulsion at 70 °C under nitrogen protection. The reaction was terminated after 4 h by quenching in ice bath. The obtained copolymer PMBV was dried in fume hood overnight and was further dried in vacuum oven at 60 °C for 24 h.

The molecular weight of the PMBV copolymers was determined by gel permeation chromatography (GPC, Waters 2410 refractive-index detector, Polymer Labs mixed-bed column ranged from 500 to 10 000 000 g $\cdot$ mol^{-1}). The composition of the obtained copolymer was determined by ^{1}H NMR spectroscopy (Bruker DRX-400 high resolution). T_g of the copolymer was determined by DSC (TA Instruments Q100).

AAEM Preparation and Characterization

The obtained PMBV was dissolved in dimethylformamide (DMF) at 40 °C followed by being quaternized by bubbling trimethylamine (Sigma-Aldrich) through the solution for 2 h with stirring. The quaternized PMBV (QPMBV) solution was then cast on an aluminum foil, and then dried in the hood for 24 h and consecutively dried in vacuum oven at 60 °C for another 24 h. The obtained QPMBV-AAEM membrane was peeled off from the aluminum foil and soaked in KOH solution (6 mol $\cdot$ L^{-1}) overnight to exchange Cl^- to OH^- form. The OH^- exchanged QPMBV-AAEM membrane was washed with DI water until pH of 7 was reached.

The ion-exchange capacity (IEC) of the QPMBV-AAEM membrane was measured by acid-based back-titration. To perform the measurement, the QPMBV-AAEM was soaked in standardized HCl water solution (0.01 mol $\cdot$ L^{-1}, 30 mL) for 1 d to ensure the complete neutralization of OH^- in the membrane. The IEC value was then determined from back-titration of the excess HCl with NaOH solution (0.01 mol $\cdot$ L^{-1}), which can be calculated by the following equation:

$$\mathrm{IEC} = \frac{(V_{\mathrm{HCl}} - V_{\mathrm{NaOH}}) \times C}{m_{\mathrm{dry}}} (\mathrm{mmol} \cdot \mathrm{g}^{-1}) \quad (1)$$

where V_{HCl} is the volume of HCl solution for membrane soaking; V_{NaOH} is the volume of NaOH solution used in back-titration; C the concentration of HCl and NaOH solution in mol $\cdot$ L^{-1}, and m_{dry} is the mass of the dry membrane.

To test the chemical stability of the membrane in high-pH environment, we measured the IEC of one representative membrane QPMBV-3 (MMA/BA/VBC = 78:5:17) in 6 M KOH solution as a function of time at room temperature. The experiment was carried out as follows: a number of QPMBV-3 membranes were kept in 6 M KOH solution at room temperature. For the IEC measurement, one membrane was taken out of the KOH solution after certain interval, and washed by de-ionized water to pH = 7. The IEC of the washed membrane was then determined by titration described above.

The water uptake was determined by gravimetry.

$$\mathrm{Water\ uptake} = \frac{M_{\mathrm{wet}} - M_{\mathrm{dry}}}{M_{\mathrm{dry}}} \times 100\% \quad (2)$$

Tensile test was conducted on dynamic mechanical analyzer (DMA, TA Instruments Q800) at room temperature to measure the Young's modulus. The stretch rate was 1 N $\cdot$ min^{-1}. Thermogravimetric analysis (TGA, TA Instruments Q500) was used to characterize the thermal stability of the obtained QPMBV-AAEMs. The heating rate was 10 °C $\cdot$ min^{-1} under nitrogen protection from room temperature to 600 °C.

Anionic conductivity was measured using electrochemical impedance spectroscopy (EIS, Gamry Instruments 3000) in the conductivity cell (BekkTech, BT-112). The temperature and relative humidity (RH) in the conductivity cell were controlled using the fuel cell test station (Arbin). Conductivity was calculated by the following equation:

$$\sigma = \frac{l}{Rab} \quad (3)$$

where l is the membrane thickness, a the membrane width, b the membrane length, and R is the resistance obtained from EIS.

Membrane Electrode Assembly (MEA) Fabrication and Performance Test

A piece of carbon paper (Toray, TGP-H-60) was firstly brushed with polytetrafluoroethylene (PTFE)/carbon black (35:65 wt%) slurry

($0.2 \pm 0.02\ mg \cdot cm^{-2}$). The carbon-supported Pt catalyst (Pt/C, 60:40 wt%) was dispersed in a dilute OH^- exchanged QPMBV solution in ethanol/water mixture (50:50 vol%) by sonication. This catalyst dispersion was sprayed onto the processed carbon paper with the Pt loading of $0.4 \pm 0.05\ mg \cdot cm^{-2}$ to form an electrode. Then, the QPMBV-AAEM membrane was sandwiched by two 5 cm^2 catalyst-loaded electrodes by hot-press (Carver 973214A) under a pressure of 2 atm at 60 °C for 10 min to obtain the MEA for fuel cell performance test.

Polarization performance was carried out on the Arbin fuel cell station. Hydrogen and oxygen with 1 atm back pressure were used as the fuel and oxidant respectively at 100 ± 2 sccm (standard $cm^3 \cdot min^{-1}$).

Results and Discussion

Characterization of PMBVs

Three PMBV copolymers with different compositions, denoted as PMBV-1, PMBV-2, and PMBV-3, were synthesized. The composition, molecular weight, and glass transition temperature of the obtained PMBVs are listed in Table 1. Composition of the PMBV copolymers was determined from ^1H NMR spectra. Chemical shifts of $\delta = 4.538$ (s, 2H, $-CH_2Cl$),[18] 3.983 (s, 2H, $-OCH_2-$),[19] and 3.588 (t, 3H, $-OCH_3$)[20] are the characteristic peaks for VBC, BA, and MMA, respectively. Since the characteristic peaks indicated the components in the copolymer, the integrated peak area can be used to calculate the composition of the PMBVs.[15] Due to the high yield of the monomers in miniemulsion copolymerization, the synthesized PMBVs have very consistent composition with the monomer ratios as shown in Table 1. The molecular weight of all three PMBV copolymers, as shown in Table 1, are all above $10^6\ g \cdot mol^{-1}$, which is almost one order of magnitude higher than those in our previous work by solution polymerization.[13] The improvement in molecular weight is attributed to the robust miniemulsion copolymerization process, and it is vital to improve the AAEM durability for fuel cell operation as discussed later in details. The results in Table 1 clearly indicate that this miniemulsion copolymerization technique enables synthesis of high molecular weight copolymer and enables precise control of the copolymer composition.

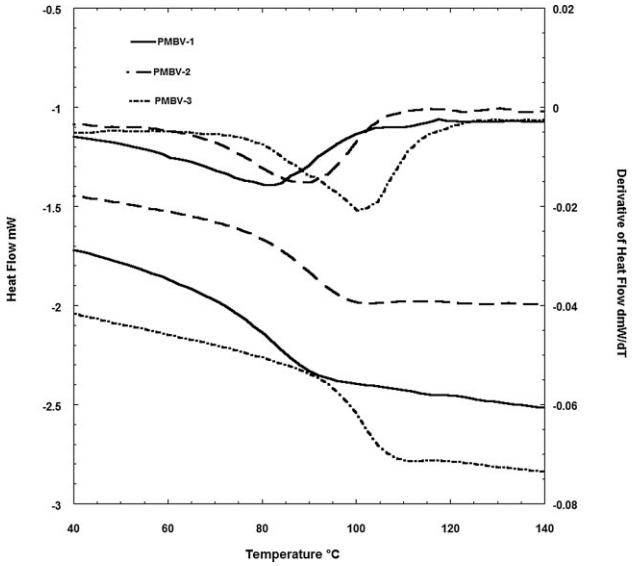

Figure 2. DSC spectra of PMBVs.

AAEMFCs are typically operated in elevated temperatures under 80 °C, it is obviously essential to have an AAEM in glassy state (below T_g) during operation to achieve high durability. The glass transition temperature (T_g) of polymer refers to a temperature below which the polymer chains will have low mobility resulting in higher mechanical strength.[20] In a temperature higher than T_g, polymers will transfer to rubbery state in which polymer chains are in segmental motion, thus leading to unstable mechanical properties. T_g of the obtained PMBV copolymers were measured by DSC as shown in Figure 2, and are listed in Table 1. The measured T_g results are consistent with the predicted values from the copolymer compositions using Equation 4.[20]

$$\frac{1}{T_g} = \frac{W_{MMA}}{T_{gMMA}} + \frac{W_{BA}}{T_{gBA}} + \frac{W_{VBC}}{T_{gVBC}} \quad (4)$$

where W with subscript is the mass ratio of each component in the polymer, and T_g with subscript represents the glass transition temperature of the corresponding homopolymers.

Table 1. Properties of PMBV copolymers via miniemulsion polymerization.

Sample	MMA/BA/VBC [mol%]		MW [$g \cdot mol^{-1}$]	T_g [°C]	
	Feed	Copolymer		Exp.	Equation 4
PMBV-1	80:10:10	75:12:13	2.3×10^6	82	78.1
PMBV-2	75:10:15	71:11:18	1.8×10^6	87	80.0
PMBV-3	80:5:15	78:5:17	1.5×10^6	101	94.3

Homopolymers of MMA and VBC are both glassy polymers with similar T_g above 100 °C, and homopolymers of BA has a significantly lower T_g at about −49 °C. PMBV-1 and PMBV-2 copolymers have very similar percentage of BA content, 12 and 11 mol% respectively, which resulted in similar T_g (82 and 87 °C) of these two copolymers. On the contrary, copolymer PMBV-3 has distinct lower BA content (5 mol%), resulting in much higher T_g of 101 °C.

Characterization of QPMBVs

QPMBV-AAEM membranes were obtained by successive steps including quaternization of PMBV copolymers, film casting, ion-exchanging, and washing-drying process. The thickness of all membranes was controlled at 50 μm using an adjustable casting blade. The quaternization degree of VBC in QPMBV-AAEMs was evaluated using combustion elemental analysis.[21] The combustion elemental analysis demonstrated a completion of quaternization (all VBC groups were quaternized) after 2 h of quaternization. The obtained QPMBV-AAEMs were transparent colorless membranes with little swelling in KOH solution (6 mol · L^{-1}). The properties of QPMBV-AAEMs are listed in Table 2.

The IEC results in Table 2 showed that QPMBV-2 and QPMBV-3 had the similar concentrations of OH^- in the membrane. Also, the OH^- concentrations in QPMBV-2 and QPMBV-3 are considerably higher than that in QPMBV-1. The IEC results are consistent to the membrane compositions, as QPMBV-2 and QPMBV-3 had similar (17 and 18 mol%, respectively) quaternized VBC groups. Meanwhile QPMBV-1 has 5 mol% less VBC than QPMBV-2 and QPMBV-3. The IEC of QPMBV-3 as a function of time in 6 M KOH is plotted in Figure 3, which shows a slight 3.3% decrease of IEC after 7 d in 6 M KOH solution. This observation indicates that the quaternary ammonium sites in the QPMBV membranes are stable in high-pH solution.

The large difference of water uptakes of these three QPMBV-AAEMs in Table 2 is attributed to their difference in IEC, molecular weight, and composition. For instance, the large difference of water uptakes between QPMBV-1 (44.6 wt%) and QPMBV-2 (197.5 wt%) is not solely attributed to the modest difference of IECs of QPMBV-1 (1.12 mmol · g^{-1}) and QPMBV-2 (1.32 mmol · g^{-1}). The higher molecular weight of QPMBV-1 (2.3×10^6 g · mol^{-1} for QPMBV-1 and 1.8×10^6 g · mol^{-1} for QPMBV-2) also contributes to the difference in water uptakes. Higher molecular weight resulted in less water uptake of the QPMBV-AAEM membrane. Comparing QPMBV-2 with QPMBV-3, in this case the difference of their IECs is even smaller, 1.32 and 1.28 mmol · g^{-1}, respectively. Therefore, the much higher water uptake of QPMBV-3 membrane is induced by a combination of its lower molecular weight, and its higher MMA content (78 mol%) and lower BA content (5 mol%) than QPMBV-2 (71 and 11 mol% of MMA and BA, respectively). As monomers, the solubility of MMA in water is 15 g · L^{-1},[22] which is ten times higher than the water solubility of BA that is 1.4 g · L^{-1}.[22] Therefore, higher water uptake of QPMBV-3 membrane was induced by more MMA and less BA composition, and lower molecular weight. The high water uptakes of QPMBV-2 and QPMBV-3 could be drastically reduced by crosslinking

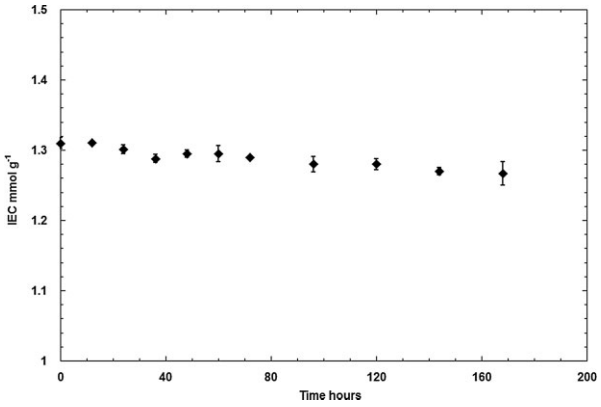

Figure 3. IEC of a QPMBV-3 membrane as a function of time in 6 M KOH at room temperature.

Table 2. Properties of QPMBV-AAEMs.

Sample	Thickness [μm]	IEC [mmol · g^{-1}]	Young's modulus [MPa]	Water uptake[a)] [wt%]	Dimensional swelling ratio[a)] [%]		
					Length	Width	Thickness
QPMBV-1	50	1.12	1330	44.6	7.8	17.3	85.7
QPMBV-2	50	1.32	1770	197.5	38.5	52.1	116.7
QPMBV-3	50	1.28	1630	325	31.6	29.0	91.7

[a)]The water uptake and dimensional change of the QPMBV membranes were measured at room temperature and fully water saturated condition.

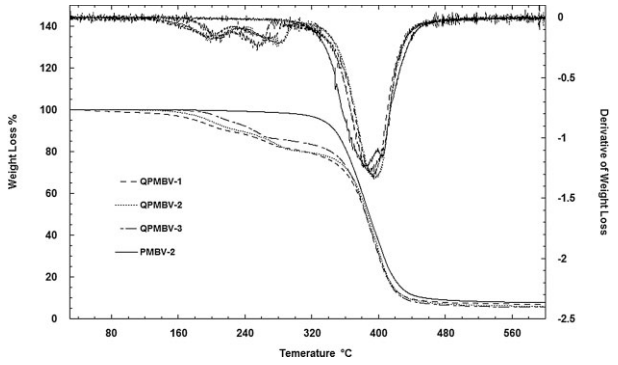

Figure 4. TGA curves of PMBV and QPMBV copolymers.

process using divinylbenzene as the crosslinking agent, without scarifying the anionic conductivity. The crosslinking mechanism is currently under investigation in our laboratory.

The thermal stability of the QPMBV-AAEMs was characterized by the TGA as shown in Figure 4. The weight loss versus temperature curve for a precursor polymer, PMBV-2, is also shown in Figure 4 as comparison. The only weight loss for PMBV-2 took place at 390 °C, which was due to the degradation of polymer chains. For the QPMBV-AAEMs, they all followed the similar weight loss transition patterns. The first transitions all began from 160 to 240 °C, which was probably corresponded to the removal of $-CH_3$ on the quaternary ammonium groups.[23] The successive weight loss transition was from 240 to 310 °C, which was due to the removal of quaternary ammonium groups from polymer chains.[7] The last visible weight loss transition was around 390 °C, indicating the decomposition of QPMBV polymer chains. The TGA analysis indicated that the QPMBV-AAEMs were thermally stable under 160 °C without degradation of the functional groups. The thermal stability of our QPMBV-AAEMs is similar to AAEMs synthesized from chloromethylation of phenyl structured polymers including poly(arylene ether sulfone) (QAPSF)[6f] and chloroacetylated poly(2,6-dimethyl-1,4-phenylene oxide) with bromomethylated poly(2,6-dimethyl-1,4-phenylene oxide).[11] The mechanical strength of QPMBV-AAEMs was also measured by tensile test using DMA. The high Young's modulus (>1 GPa) of our QPMBV-AAEMs was comparable to those synthesized from chloromethylation of polysulfone (QAPS).[6b]

The conductivities of QPMBV-AAEMs are shown in Figure 5. The temperature and humidity were controlled using Arbin fuel cell test station as same as the fuel cell performance testing. The conductivity increased as the temperature went up from 50 to 80 °C. QPMBV-2 and QPMBV-3 could reach the highest conductivity around 4×10^{-2} S · cm^{-1} at 80 °C with 80% RH, while the highest conductivity of QPMBV-1 was 1.9×10^{-2} S · cm^{-1} at the same conditions. The twofold lower conductivity of

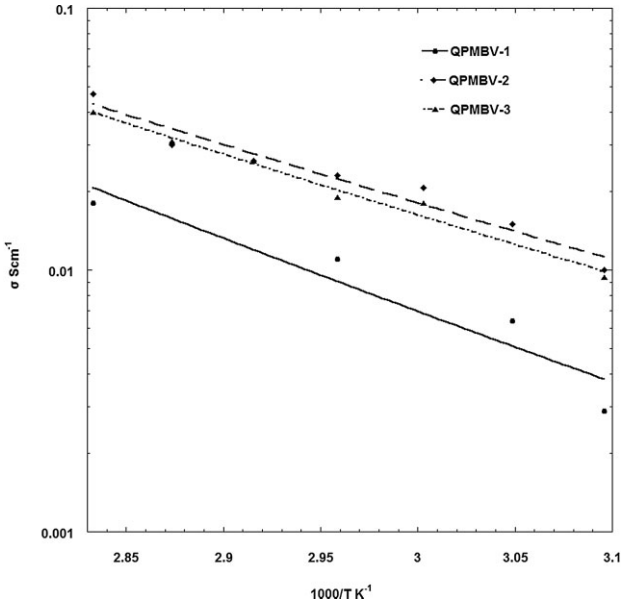

Figure 5. Conductivities for QPMBVs at 80% RH.

QPMBV-1 was due to its lower IEC and lower water uptake. The high conductivity of our QPMBV-AAEMs, especially QPMBV-2 and QPMBV-3, was better than that of the AAEMs synthesized by chloromethylation of poly(2,6-dimethyl-1,4-phenylene oxide) (0.035 S · cm^{-1} at 90 °C),[14c] poly(tetrafluoroethene-*co*-hexafluropropylene) (0.03 S · cm^{-1} fully hydrated at 30 °C),[14d] and polysulfone/methylene quaternary phosphonium hydroxide (TPQPOH, 0.027 S · cm^{-1} fully hydrated at 30 °C).[6d] The activation energy of our QPMBV-AAEMs is around 50 kJ · mol^{-1}, which is similar to the quaternized poly(arylene ether sulfone) (QPASF) AAEMs (43.8 kJ · mol^{-1}).[8] Both mechanical properties and conductivities indicated our tuned QPMBV-AAEM as a great candidate for AAEMFC application.

Fuel Cell Performance

With the demonstrated high mechanical strength and anionic conductivity, exceptional fuel cell performance can be expected from the QPMBV-AAEM fuel cells.

Figure 6 and 7 are the polarization performances of AAEMFCs using QPMBV-AAEMs. The performance of QPMBV fuel cell was increased with increasing temperature. The QPMBV-3 membrane delivered peak power density of 180 mW · cm^{-2} at 0.45 V and maximum current density of 500 mA · cm^{-2} at 70 °C. The deliverable power density of the QPMBV-AAEMs was 80 mW · cm^{-2} higher than that of QAPS membranes,[6b,6e] and was also comparable to that of TPQPOH membranes (250 mW · cm^{-2}),[6f] however, which was achieved with a much higher back pressure (3 atm). The relatively lower power output of QPMBV-1 is due to its lower anionic conductivity as

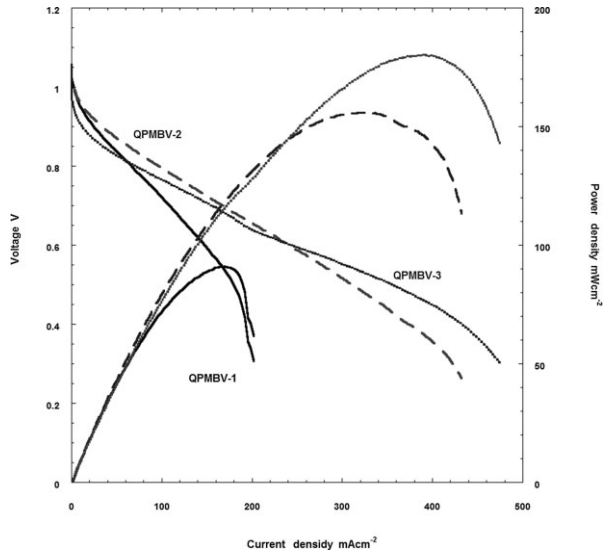

Figure 6. Polarization curves for QPMBVs at 70 °C and 80% RH.

described previously. The polarization performance of QPMBV-3 is also better than QPMBV-2 due to its lower BA content and higher MMA content. As previously mentioned, more relatively hydrophilic composition of QPMBV-3 membrane could attract more water thus facilitating polarization performance. As shown in Figure 6, QPMBV-2, with 6 mol% more BA and 7 mol% less MMA comparing with QPMBV-3, showed a slightly higher Ohmic loss and a clearly earlier concentration loss. Same behavior was also observed in Figure 7 at a lower temperature of 60 °C.

Besides the temperature effect, RH effects on the polarization behavior of AAEMFCs were also investigated.

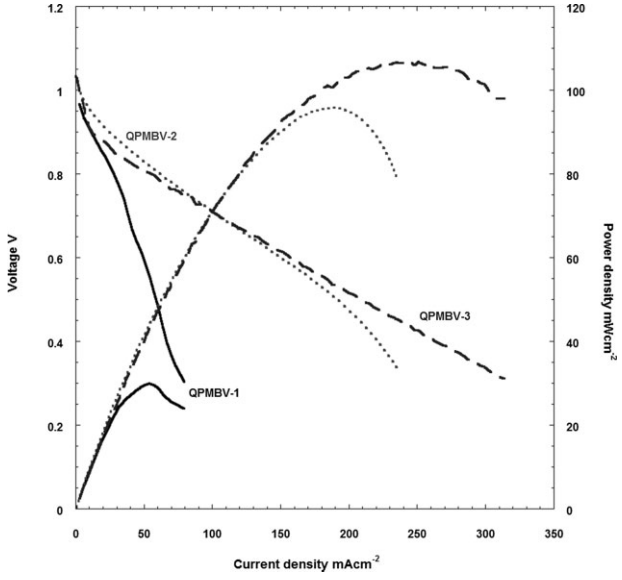

Figure 7. Polarization curves for QPMBVs at 60 °C and 80% RH.

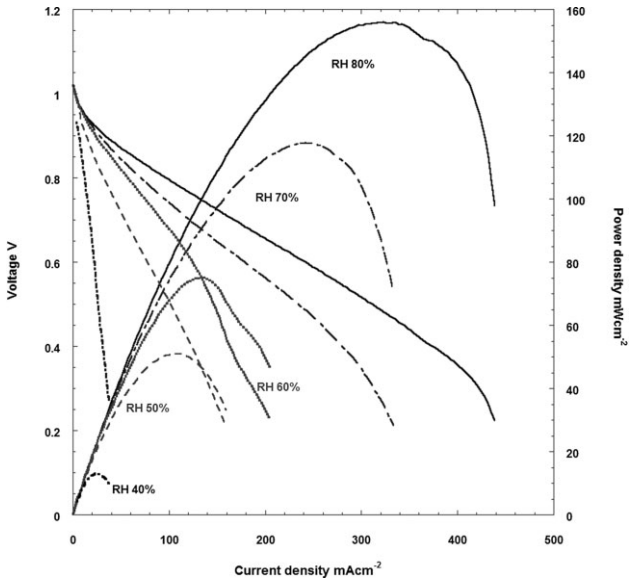

Figure 8. Polarization curves of QPMBV-2 at 70 °C and different RH.

It was shown in Figure 8 that lower RH resulted in decreased performance of AAEMFCs, as both Ohmic loss and concentration loss exacerbated. This distinct dependency on RH illustrated that water retention is important for OH^- transport in AAEM membranes. To ensure an energy density higher than 50 $mW \cdot cm^{-2}$ in our AAEMFC system, minimum 50% RH was required.

To date, little investigation on membrane durability has been conducted on AAEMFCs. However, this test is of great importance for the long term prospect of AAEMFCs. In this study, the effect of different compositions on durability of QPMBV-AAEMs was tested. Specifically, QPMBV-2 and QPMBV-3 were tested at the current density of 200 $mA \cdot cm^{-2}$, and QPMBV-1 was tested at the current density of 100 $mA \cdot cm^{-2}$ due to its lower current at the peak power density. From Figure 9, the corresponding stable voltage was around 0.7 V, which was consistent to the data

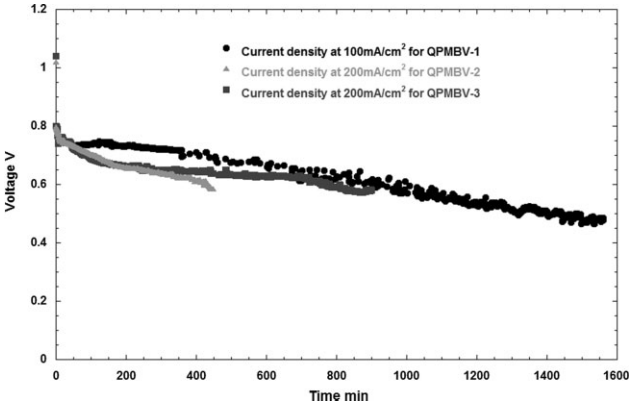

Figure 9. Durability test for QPMBVs at 70 °C and 80% RH.

shown in the polarization curves in Figure 6. The durability performance showed that QPMBV-3 could deliver stable current for 15 h while QPMBV-2 could deliver 8 h with same operating conditions and very similar conductivities. The better durability of QPMBV-3 comparing with QPMBV-2 is attributed to its higher glass transition temperature, i.e., a more rigid AAEM in the working environment could help improving the durability. The QPMBV-1 membrane delivered the best durability performance despite the lower current density. It was shown in Figure 9 that 26 h of stable current delivering was achieved by QPMBV-1. This was obviously due to its less VBC content, i.e., water uptake, as well as the highest MW among these three membranes.

Conclusion

A series of QPMBV-AAEMs were synthesized with designed composition using miniemulsion copolymerization. This unique polymerization technique can precisely tune the composition by monomer ratio adjustment, which in turn could balance the mechanical properties and conductivity of the resulted AAEMs. Moreover, it can be used to synthesize high molecular weight QPMBVs to enhance the mechanical properties. Our QPMBV-AAEMs demonstrated one of the best over-all performance including high deliverable power density and durability. Moreover, the simple and robust synthesis technique and low cost materials provide a promising alternative to current AAEM technologies.

The effects of the QPMBV-AAEM composition on the membrane properties and their fuel cell performances can be summarized as follows: (i) higher molecular weight can improve the mechanical strength of the membrane, as well as reducing the water uptake; (ii) higher concentration of the anionic conductive sites (i.e., VBC in our membranes) can improve the conductivity but at same time impairing the mechanical properties; (iii) increasing the glass transition temperature of the copolymer by lowering the low T_g content can improve the membrane durability working at elevated temperatures; and (iv) the water hydrophilicity of the non-conductive portion (mechanical support) of the membrane is also of great importance to the water uptake, i.e., mechanical strength of the AAEM membranes. Therefore, due to these complex composition effects, one particular AAEM membrane should be precisely designed and synthesized to optimize its performance. For instance, MMA can be replaced by another monomer with similar or higher polymer glass transition temperature and less hydrophilicity. Meanwhile, the feasibility of achieving high molecular weight and the processability of the copolymer has to be considered. For this particular QPMBV-AAEM system, to further enhance both mechanical strength and conductivity, an interpolymer network (IPN) will be applied to make the crosslinked QPMBV-AAEM membranes. The crosslinking agent will be used to improve the mechanical support by holding QPMBV in the network. More VBC could be incorporated into the QPMBV matrix to enhance the conductivity without sacrificing the mechanical strength. This study is being carried out in our laboratory.

Acknowledgements: This research was supported by the Office of Naval Research (N000140810717), the Army Research Lab (W911NF0920007), and the Army Research Office (W911NF0910028). The authors are grateful to Prof. P. Kofinas at the University of Maryland for the technical support.

Received: April 11, 2011; Revised: June 15, 2011; Published online: August 24, 2011; DOI: 10.1002/macp.201100218

Keywords: alkaline anion-exchange membranes; emulsion polymerization; fuel cells; membranes; polymer electrolytes

[1] N. J. Robertson, H. A. Kostalik, IV, T. J. Clark, P. F. Mutolo, H. D. Abruna, G. W. Coates, *J. Am. Chem. Soc.* **2010**, *132*, 3400.
[2] R. O'Hayre, S. W. Cha, W. Colella, F. B. Prinz, *Fuel Cell Fundamentals*, John Wiley & Sons, New York, USA **2006**.
[3] Y. Wu, C. Wu, F. Yu, T. Xu, Y. Fu, *J. Membr. Sci.* **2008**, *307*, 28.
[4] V. M. Nikolic, A. Krkljes, Z. K. Popovic, Z. V. Lausevic, S. S. Miljanic, *Electrochem. Commun.* **2007**, *9*, 2661.
[5] G. M. Wu, S. J. Lin, C. C. Yang, *J. Membr. Sci.* **2006**, *275*, 127.
[6] a) G. Wang, Y. Weng, D. Chu, R. Chen, D. Xie, *J. Membr. Sci.* **2009**, *333*, 63; b) S. Lu, J. Pan, A. Huang, L. Zhuang, J. Lu, *Proc. Natl. Acad. Sci. USA* **2008**, *105*, 20611; c) J. Zhou, M. Unlu, V. A. Vega, P. A. Kohl, *J. Power Sources* **2009**, *190*, 285; d) S. Gu, R. Cai, T. Luo, Z. Chen, M. Sun, Y. Liu, G. He, Y. Yan, *Angew. Chem. Int. Ed.* **2009**, *48*, 6499; e) J. Pan, S. Lu, Y. Li, A. Huang, L. Zhuang, J. Lu, *Adv. Funct. Mater.* **2010**, *20*, 312; f) S. Gu, R. Cai, T. Luo, K. Jensen, C. Contreras, Y. Yan, *ChemSusChem* **2010**, *3*, 555.
[7] Y. Xiong, Q. Liu, Q. Zeng, *J. Power Sources* **2009**, *193*, 541.
[8] G. Wang, Y. Weng, J. Zhao, R. Chen, D. Xie, *J. Appl. Polym. Sci.* **2009**, *112*, 721.
[9] L. Li, Y. Yang, *J. Membr. Sci.* **2005**, *262*, 1.
[10] J. Fang, P. Shen, *J. Membr. Sci.* **2006**, *285*, 317.
[11] L. Wu, T. Xu, D. Wu, X. Zheng, *J. Membr. Sci.* **2008**, *310*, 577.
[12] M. R. Hibbs, C. H. Fujimoto, C. J. Cornelius, *Macromolecules* **2009**, *42*, 8316.
[13] E. E. Switzer, T. S. Olson, A. K. Datye, P. Atanassov, M. R. Hibbs, C. Fujimoto, C. J. Conelius, *Electrochim. Acta* **2010**, *55*, 3404.
[14] a) J. R. Varcoe, R. C. T. Slade, E. L. H. Yee, S. D. Poynton, D. J. Priscoll, D. C. Apperley, *Chem. Mater.* **2007**, *19*, 2686; b) T. N. Danks, R. C. T. Slade, J. R. Varcoe, *J. Mater. Chem.* **2003**, *13*, 712; c) Y. Wu, C. Wu, J. R. Varcoe, S. D. Poynton, T. Xu, Y. Fu, *J. Power Sources* **2010**, *195*, 3069; d) J. R. Varcoe, *Phys. Chem. Chem. Phys.* **2007**, *9*, 1479.

[15] Y. Luo, J. Guo, C. Wang, D. Chu, *J. Power Sources* **2010**, *195*, 3765.
[16] a) J. Reimrs, F. J. Schork, *J. Appl. Polym. Sci.* **1996**, *59*, 1833; b) F. J. Schork, J. Guo, *Macromol. React. Eng.* **2008**, *2*, 287.
[17] J. Guo, F. J. Schork, *Macromol. React. Eng.* **2008**, *2*, 265.
[18] J. F. Quinn, R. P. Chaplin, T. P. Davis, *J. Polym. Sci., Part A: Polym. Chem.* **2002**, *40*, 2956.
[19] a) P. Paris, J. Fuenta, *J. Polym. Sci., Polym. Chem.* **2007**, *45*, 2538; b) M. A. Dube, A. Penlidis, *Polymer* **1995**, *36*, 587.
[20] J. E. Mark, A. Eisenberg, W. W. Graessley, L. Mandelkern, E. T. Samulski, J. L. Koenig, G. D. Wignall, *Physical Properties of Polymers*, United Book Press, Baltimore, USA **1993**.
[21] Y. Luo, J. Guo, C. Wang, K. Y. Choi, D. Chu, *ECS Trans.* **2010**, *33*, 1893.
[22] A. Ziegler, K. Landfester, A. Musyanovych, *Colloid Polym. Sci.* **2009**, *287*, 1261.
[23] G. Wang, Y. Weng, D. Chu, D. Xie, R. Chen, *J. Membr. Sci.* **2009**, *326*, 4.